Contribution from the Department of Chemistry,
The Pennsylvania State University, University Park, Pennsylvania 16802

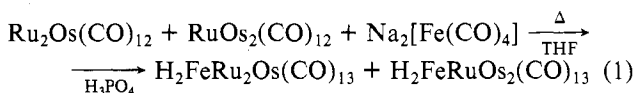# Synthesis of Tetranuclear Mixed-Metal Clusters via the Reaction of [Co(CO)4]− with Closed Metal Carbonyl Trimers. Crystal and Molecular Structure of [(Ph3P)2N][CoRu3(CO)13]

PAUL C. STEINHARDT, WAYNE L. GLADFELTER, A. DALE HARLEY, JOSEPH R. FOX, and GREGORY L. GEOFFROY*

The new clusters $HCoRu_3(CO)_{13}$, $HCoRu_2Os(CO)_{13}$, $HCoRuOs_2(CO)_{13}$, and $HCoOs_3(CO)_{13}$ have been synthesized by allowing $K[Co(CO)_4]$ to react with $Ru_3(CO)_{12}$, $Ru_2Os(CO)_{12}$, $RuOs_2(CO)_{12}$, and $Os_3(CO)_{12}$, respectively, followed by protonation. Reaction of $K[Co(CO)_4]$ with $Fe_3(CO)_{12}$, $Fe_2Ru(CO)_{12}$, and $FeRu_2(CO)_{12}$ followed by acidification did not lead to the desired hydrido mixed-metal clusters but instead to various other products. Reaction of [PPN][Co(CO)_4] (PPN = (Ph3P)2N) with $Fe_3(CO)_{12}$ and $Ru_3(CO)_{12}$ without subsequent acidification gave the salts $[PPN][CoFe_3(CO)_{13}]$ and $[PPN][CoRu_3(CO)_{13}]$. The latter was structurally characterized by single-crystal X-ray diffraction. It crystallizes in the space group $P\bar{1}$ with $Z = 2$ and unit cell dimensions $a = 9.783$ (5) Å, $b = 14.768$ (5) Å, $c = 18.675$ (5) Å, $\alpha = 110.39$ (3)°, $\beta = 99.02$ (4)°, $\gamma = 91.44$ (4)°, and $V = 2489$ (4) Å^3. Diffraction data ($0° < 2\theta \leq 50°$) were collected with an Enraf-Nonius CAD4 automated diffractometer, using graphite-monochromatized Mo $K\alpha$ radiation, and the structure was refined to $R = 0.036$ and $R_w = 0.044$ for 6150 independent reflections with $I \geq 3.0\sigma(I)$. The molecule contains a tetrahedral $CoRu_3$ core with each Ru atom bonded to three terminal carbonyls, the Co atom bonded to one terminal carbonyl, and a carbonyl ligand bridging each of the three Co–Ru bonds. Analogous reactions of $[PPN][Co(CO)_4]$ with $Fe_2Ru(CO)_{12}$ and $FeRu_2(CO)_{12}$ gave products formulated as $[PPN][CoFe_2Ru(CO)_{13}]$ and $[PPN][CoFeRu_2(CO)_{13}]$, but these salts were not obtained pure.

We have previously demonstrated[1] a useful synthetic route to tetranuclear mixed-metal clusters of the Fe–Ru–Os triad by the addition of carbonylmetalates to closed metal carbonyl trimers. For example, addition of $[Fe(CO)_4]^{2-}$ to $Ru_2Os(CO)_{12}$ and $RuOs_2(CO)_{12}$ gave the trimetallic clusters $H_2FeRu_2Os(CO)_{13}$ and $H_2FeRuOs_2(CO)_{13}$, eq 1.

$$Ru_2Os(CO)_{12} + RuOs_2(CO)_{12} + Na_2[Fe(CO)_4] \xrightarrow[\text{THF}]{\Delta}$$
$$\xrightarrow[H_3PO_4]{} H_2FeRu_2Os(CO)_{13} + H_2FeRuOs_2(CO)_{13} \quad (1)$$

We are currently evaluating the scope of this synthetic approach by varying the nature of the carbonylmetalates and the metal trimers. Tetracarbonylcobaltate has been found to work well in these reactions, and we report herein the synthesis and characterization of the new clusters $HCoRu_3(CO)_{13}$, $HCoRu_2Os(CO)_{13}$, $HCoRuOs_2(CO)_{13}$, $HCoOs_3(CO)_{13}$, $[CoRu_3(CO)_{13}]^-$, and products tentatively formulated as $[CoFeRu_2(CO)_{13}]^-$ and $[CoFe_2Ru(CO)_{13}]^-$. Details concerning the preparation of $[CoFe_3(CO)_{13}]^-$, a cluster previously prepared by Chini and co-workers,[2] are also given.

Experimental Section

$Co_2(CO)_8$, $Ru_3(CO)_{12}$, $Os_3(CO)_{12}$, and [PPN]Cl were obtained from Alfa Ventron Corp. and were used without further purification. $Fe_3(CO)_{12}$,[3] $Fe_2Ru(CO)_{12}$,[4] $FeRu_2(CO)_{12}$,[4] $Ru_2Os(CO)_{12}$,[5] and $RuOs_2(CO)_{12}$[5] were prepared according to published procedures. Tetrahydrofuran (THF), hexane, and 1,2-dimethoxyethane were dried by distillation from sodium benzophenone ketyl or CaH_2 under N_2. MeOH and EtOH were dried by distillation from $Mg(OMe)_2$ and $Mg(OEt)_2$, respectively, 2-ethoxyethanol was dried by distillation from $MgSO_4$, and CH_2Cl_2 was dried by distillation from P_4O_{10} under N_2. All other solvents were used as obtained. Solutions of the reactants were prepared in an N_2-filled drybox, and all reactions were carried out under an N_2 atmosphere. Unless otherwise stated, the inert atmosphere was maintained up to the point of the first hexane extraction following acidification. Chromatography was conducted on

silica gel with the low-pressure chromatography apparatus previously described.[1] For air-sensitive compounds, the silica gel was deoxygenated by passing ~1 L of dried, deoxygenated solvent through the column prior to chromatography of the reaction mixtures. The fractions were collected under N_2 in Schlenk flasks, and the solvent was removed by evaporation under vacuum.

Preparation of K[Co(CO)4] Solutions.[6] Approximately 1 mL of NaK alloy (1:2.8) was added by syringe to a 75-mL THF solution of $Co_2(CO)_8$ (0.1 g, 0.29 mmol). After being stirred at 25 °C for ~3 h the solution was faint purple or blue with a suspended gray precipitate. The solution was then filtered under an N_2 atmosphere with Schlenk techniques to obtain a colorless or occasionally pale yellow solution of $K[Co(CO)_4]$. This $K[Co(CO)_4]$ solution was used immediately in the reactions described below, and no attempts were made to isolate solid $K[Co(CO)_4]$.

Preparation of [PPN][Co(CO)4]. This salt was prepared by an adaptation of the literature procedure.[7] A 75-mL THF solution of $Co_2(CO)_8$ (1.7 g, 5 mmol) was reduced with 2 mL of NaK alloy and filtered as described above. Addition of [PPN][Cl] (5.193 g, 9.04 mmol) in 50 mL of CH_2Cl_2 to the filtrate gave a light green precipitate which was isolated by filtration. Recrystallization from CH_2Cl_2/Et_2O gave light green crystals of $[PPN][Co(CO)_4]$ (4.456 g, 6.28 mmol).

Preparation of HCoRu3(CO)13. 1. A 60-mL THF solution of $Ru_3(CO)_{12}$ (100 mg, 0.156 mmol) was added dropwise over a 30-min period to a refluxing and stirred 60-mL THF solution of $K[Co(CO)_4]$ (by reduction of 0.1 g, 0.29 mmol of $Co_2(CO)_8$). After heating of the mixture for an additional 2 h, solvent was removed from the resultant deep red solution by evaporation under vacuum. A 60-mL portion of deoxygenated hexane was then added followed by 40 mL of a deoxygenated 20% aqueous H_3PO_4 solution. The acid layer was extracted with 60-mL portions of hexane (360-mL total) until colorless. The red hexane solution was dried over anhydrous $MgSO_4$, filtered, concentrated, and chromatographed on silica gel. With hexane as the eluent at 50 lb column pressure, a yellow band containing $Ru_3(CO)_{12}$ with a trace of $H_2Ru_4(CO)_{13}$ and a brown band of $HCoRu_3(CO)_{13}$ (72 mg, 63% yield) eluted in that order. The pure compound was obtained as slightly air-sensitive red microcrystals by evaporation of solvent. Anal. Calcd for $HCoRu_3(CO)_{13}$: C, 21.47; H, 0.14. Found: C, 21.42; H, 0.14 (Galbraith Laboratories).

2. A 50–60% yield of $HCoRu_3(CO)_{13}$ can be obtained without chromatography by first washing the H_3PO_4 acidified reaction mixture (see above) two or three times with hexane to remove remaining

(1) Geoffroy, G. L.; Gladfelter, W. L. *J. Am. Chem. Soc.* **1977**, *99*, 7656.
(2) Chini, P.; Heaton, B. T. *Top. Curr. Chem.* **1977**, *71*, 1.
(3) McFarlane, W.; Wilkinson, G. *Inorg. Synth.* **1966**, *8*, 181.
(4) Yawney, D. B. W.; Stone, F. G. A. *J. Chem. Soc. A* **1969**, 502.
(5) Johnson, B. F. G.; Johnston, R. D.; Lewis, J.; Williams, I. G.; Kilty, P. A. *Chem. Commun.* **1968**, 861.
(6) Ellis, J. E.; Flom, E. A. *J. Organomet. Chem.* **1975**, *99*, 263.
(7) Ruff, J. K.; Schlientz, W. J. *Inorg. Synth.* **1974**, *15*, 87.

$Ru_3(CO)_{12}$ and $Co_4(CO)_{12}$, followed by extraction of the acid layer with several aliquots of benzene. After the benzene extract is dried with $MgSO_4$, evaporation of solvent leaves a red crystalline mass of pure $HCoRu_3(CO)_{13}$.

Preparation of $HCoRu_2Os(CO)_{13}$ and $HCoRuOs_2(CO)_{13}$. A 60-mL partially dissolved THF solution of the $Ru_2Os(CO)_{12}$, $RuOs_2(CO)_{12}$, $Ru_3(CO)_{12}$, and $Os_3(CO)_{12}$ mixture[5] (614 mg combined weight, ~193 mg of $Ru_2Os(CO)_{12}$, ~217 mg of $RuOs_2(CO)_{12}$[8]) was added dropwise over a 25-min period to a stirred, refluxing 100-mL THF solution of $K[Co(CO)_4]$ (by reduction of 0.6 g, 1.76 mmol of $Co_2(CO)_8$). Heating was continued for an additional 2 h and workup of the resultant red solution was similar to that described above for $HCoRu_3(CO)_{13}$, except that the reaction mixture was extracted with benzene. Benzene was removed by evaporation and the residue redissolved in hexane. Chromatography on silica gel with hexane as the eluting solvent yielded in order of elution a yellow band of the unreacted trimer mixture, a dark brown band consisting of H_4Os_4-$(CO)_{12}$, $Os_3(CO)_{12}$, and $Co_4(CO)_{12}$, a brown band of $HCoRu_3(CO)_{13}$, a dark orange band of $HCoRu_2Os(CO)_{13}$, and an orange band of $HCoRuOs_2(CO)_{13}$. Relatively pure compounds were obtained by simple evaporation of the solvent from the respective fractions giving moderate yields of $HCoRu_2Os(CO)_{13}$ (83 mg, 38%) and $HCoRu$-$Os_2(CO)_{13}$ (59 mg, 25%).

Preparation of $[PPN][CoRu_3(CO)_{13}]$. A solution of $Ru_3(CO)_{12}$ (105 mg, 0.154 mmol) and $[PPN][Co(CO)_4]$ (109 mg, 0.154 mmol) in 125 mL of dried, deoxygenated THF was refluxed for 2.5 h under N_2 during which time the color changed from yellow to dark red. Evaporation of THF gave a red solid which was dissolved in 60 mL of dried, deoxygenated Et_2O and recrystallized by slow diffusion of hexane into the Et_2O solution under vacuum to give 64% yield (124 mg) of $[PPN][CoRu_3(CO)_{13}]$. Anal. Calcd for $[PPN][CoRu_3$-$(CO)_{13}]$: C, 46.53; H, 2.40; Ru, 23.97. Found: C, 46.55; H, 2.38; Ru, 23.65 (Alfred Bernhardt Analytical Laboratories, Engelskirchen, West Germany).

Preparation of $[PPN][CoFe_2Ru(CO)_{13}]$. A solution of $[PPN]$-$[Co(CO)_4]$ (87 mg, 0.122 mmol) and $Fe_2Ru(CO)_{12}$ (67 mg, 0.122 mmol) in 50 mL of freshly dried, deoxygenated THF was refluxed under N_2 for 2 h during which time the color changed from purple to deep red. Evaporation of THF gave a brown solid which was dissolved in Et_2O and recrystallized by slow diffusion of hexane to give a 16% yield (24 mg) of impure $[PPN][CoFe_2Ru(CO)_{13}]$. Anal. Calcd for $[PPN][CoFe_2Ru(CO)_{13}]$: C, 50.11; H, 2.58; Fe, 9.51; Ru, 8.60. Found: C, 46.88; H, 2.57; Fe, 5.75; Ru, 8.99 (Alfred Bernhardt).

Preparation of $[PPN][CoFeRu_2(CO)_{13}]$. A solution of $[PPN]$-$[Co(CO)_4]$ (53 mg, 0.755 mmol) and $FeRu_2(CO)_{12}$ (45 mg, 0.757 mmol) in 75 mL of dried, deoxygenated THF was refluxed under N_2 for 1.25 h during which time the color changed from light red to dark red. Evaporation of solvent gave a brown solid which was dissolved in 20 mL of dried, deoxygenated Et_2O and recrystallized by slow diffusion of hexane under vacuum to give a 47% yield (43 mg) of slightly air-sensitive red-brown crystals of impure $[PPN][CoFe$-$Ru_2(CO)_{13}]$. Anal. Calcd for $[PPN][CoFeRu_2(CO)_{13}]$: C, 48.25; H, 2.48; Fe, 4.57; Ru, 16.57. Found: C, 46.92; H, 2.57; Fe, 3.62; Ru, 14.69 (Alfred Bernhardt).

Preparation of $[PPN][CoFe_3(CO)_{13}]$. A solution of $[PPN][Co(C$-$O)_4]$ (251 mg, 0.495 mmol) and $Fe_3(CO)_{12}$ (250 mg, 0.496 mmol) in 125 mL of dried, deoxygenated THF was stirred under N_2 for 22 h at 25 °C during which time the color changed from dark green to red-purple. Evaporation of solvent gave a black solid which was recrystallized by dissolution in 80 mL of dried, deoxygenated Et_2O, leaving a brown impure $[PPN][Co(CO)_4]$ residue, and slow diffusion of hexane into the solution under vacuum to give an 18% yield (104 mg) of black, slightly air-sensitive crystals. Anal. Calcd for $[PPN][CoFe_3(CO)_{13}]$: C, 52.12; H, 2.68; Fe, 14.84; Co, 5.22. Found: C, 52.04; H, 2.85; Fe, 14.72; Co, 5.08 (Alfred Bernhardt).

Spectral Measurements. Infrared spectra were recorded on a Perkin-Elmer 580 infrared spectrophotometer using 0.5-mm NaCl solution infrared cells. These cells were sealed with serum caps and purged with N_2 in order to record the spectra of air-sensitive compounds. Values reported are accurate to ±1 cm⁻¹. Electron impact

---

(8) Although the trimer mixture used in this synthesis was not analyzed, we previously found[1] that the pyrolysis reaction[5] yielded a 1:2:2:1 mixture of Ru_3-, Ru_2Os-, $RuOs_2$-, and $Os_3(CO)_{12}$. The yields of $HCoRu_2Os(CO)_{13}$ and $HCoRuOs_2(CO)_{13}$ were calculated by assuming this ratio of trimers.

Table I. Data for the X-ray Diffraction Study of $[PPN][CoRu_3(CO)_{13}]$

Crystal Parameters	
cryst system: triclinic	$V = 2489$ (4) Å
space group: $P\bar{1}$	temp = 23 °C
$a = 9.783$ (5) Å	$Z = 2$
$b = 14.768$ (5) Å	mol wt = 1264.88
$c = 18.675$ (5) Å	d(calcd) = 1.688 g cm⁻³
$\alpha = 110.39$ (3)°	d(obsd) = 1.700 g cm⁻³
$\beta = 99.02$ (4)°	
$\gamma = 91.44$ (4)°	

Measurement of Intensity Data

radiation: Mo Kα (λ 0.710 73)
monochromator: graphite crystal
reflctns measd: $+h$, $\pm k$, $\pm l$
max $2\theta = 50.0°$
min $2\theta = 0°$
scan type: $\theta-2\theta$
scan speed: variable, see text
reflctns collected: 8964 unique reflctns; 6150 obsd above $3\sigma(I)$ level
std reflctns: 3 measd every 2 h (~185 reflctns); there was no significant decay over the course of the data collection

mass spectra were obtained by using an AEI-MS9 spectrometer with a source voltage maintained at 70 eV. The probe temperature varied between 100 and 200 °C depending on the cluster examined. NMR spectra were obtained by using a JEOL PS-100-FT Fourier transform spectrometer. Electronic absorption spectra were recorded on a Cary 17 spectrophotometer using 1.0-cm path length quartz cells.

Collection and Reduction of the X-ray Data for $[PPN][CoRu_3(CO)_{13}]$. Dark red crystals of $[PPN][CoRu_3(CO)_{13}]$ were grown by slow evaporation of solvent from a saturated Et_2O solution of the complex. The irregularly shaped crystal selected for analysis had maximum dimensions of 0.4 × 0.3 × 0.2 mm. It was mounted in an arbitrary orientation on a glass fiber which was then fixed into an aluminum pin and mounted onto an eucentric goniometer. Diffraction data were collected on an Enraf-Nonius four-circle CAD4 automated diffractometer controlled by a PDP8/a computer coupled to a PDP 11/34 computer. The Enraf-Nonius program SEARCH was employed to obtain 25 accurately centered reflections which were then used in the program INDEX to obtain an orientation matrix for data collection and to provide cell dimensions.[9] Pertinent crystal and intensity data are listed in Table I.

A graphite crystal incident beam monochromator was used with Mo Kα radiation, and data were collected at a takeoff angle of 2.80°. A $\theta-2\theta$ scan method was used with a variable scan rate ranging from 20°/min for the most intense reflections to 1°/min for the weak ones. The angular scan (ω) width was variable and amounted to 0.6° below 2θ(Mo Kα) and (0.6 + 0.347 tan θ) above 2θ(Mo Kα). High and low 2θ backgrounds were each scanned for 25% of the total scan time. A total of 8964 unique reflections were collected out to $2\theta = 50°$. Of these, 6150 had intensities with $I \geq 3.0\sigma(I)$ and were considered observed. (Here $\sigma(I) = [S^2(C + R^2B) + (pI)^2]^{1/2}$ and $I = S(C - RB)$ where S = scan rate, C = total integrated peak count, R = ratio of scan time to background counting time, B = total background count, and $p = 0.02$). These data were corrected for Lorentz and polarization factors and were used in the subsequent refinement of the structure.

Solution and Refinement of the Structure. Of the two possible triclinic space groups, $P1$ and $P\bar{1}$, the latter was arbitrarily selected for the initial trial solution of the structure. The successful refinement of the structure using this space group indicated that this choice was correct. The Co and three Ru atoms were located from a three-dimensional Patterson map, and the coordinates of the remaining 65 nonhydrogen atoms were located by successive least-squares refinements and difference Fourier maps. Several cycles of least-squares refinement with anisotropic temperature factors for all 69 nonhydrogen atoms reduced R to 0.036 and R_w to 0.044. The residuals are defined as

$$R = \sum(||F_o| - |F_c||)/\sum|F_o|$$

$$R_w = [\sum w(|F_o| - |F_c|)^2/\sum w|F_o|^2]^{1/2}$$

---

(9) All programs used in this study are part of the Enraf-Nonius Structure Determination Package (SDP), Enraf-Nonius, Delft, Holland, 1975, revised 1977.

Table II. Positional and Thermal Parameters and Their Estimated Standard Deviations[a]

atom	x	y	z	B_{11}	B_{22}	B_{33}	B_{12}	B_{13}	B_{23}
Ru1	0.29765 (5)	0.40496 (3)	0.27888 (2)	0.00911 (5)	0.00866 (3)	0.00286 (1)	0.00140 (6)	0.00288 (4)	0.00471 (3)
Ru2	0.03525 (4)	0.40907 (3)	0.32579 (2)	0.01052 (5)	0.00612 (2)	0.00298 (1)	0.00423 (6)	0.00505 (4)	0.00381 (2)
Ru3	0.06370 (5)	0.45057 (3)	0.19199 (2)	0.01103 (5)	0.00470 (2)	0.00303 (1)	−0.00007 (5)	0.00214 (4)	0.00373 (2)
Co1	0.08595 (7)	0.27794 (5)	0.19902 (4)	0.01145 (8)	0.00477 (3)	0.00323 (2)	0.00275 (4)	0.00442 (7)	0.00352 (4)
P1	0.3466 (1)	0.09799 (9)	0.66657 (7)	0.0082 (1)	0.00445 (7)	0.00239 (4)	0.0007 (2)	0.0025 (1)	0.00086 (8)
P2	0.3102 (1)	0.16114 (9)	0.83110 (7)	0.0096 (1)	0.00409 (6)	0.00254 (4)	0.0018 (2)	0.0031 (1)	0.00228 (7)
O1	0.0387 (7)	0.0752 (3)	0.1054 (3)	0.0462 (13)	0.0048 (3)	0.0084 (3)	−0.0003 (10)	0.0098 (10)	0.0018 (4)
O2	0.3090 (4)	0.2577 (3)	0.1137 (2)	0.0166 (5)	0.0122 (3)	0.0041 (1)	0.0088 (7)	0.0093 (4)	0.0048 (3)
O3	0.0863 (5)	0.1998 (3)	0.3199 (2)	0.0373 (8)	0.0096 (2)	0.0072 (1)	0.0202 (7)	0.0205 (5)	0.0124 (2)
O4	−0.1784 (4)	0.2875 (3)	0.1129 (2)	0.0136 (5)	0.0073 (2)	0.0073 (2)	−0.0032 (6)	−0.0024 (5)	0.0072 (3)
O5	0.5340 (5)	0.4777 (4)	0.2199 (2)	0.0173 (6)	0.0159 (4)	0.0059 (2)	−0.0049 (8)	0.0077 (5)	0.0087 (3)
O6	0.4590 (5)	0.2764 (4)	0.3496 (2)	0.0206 (7)	0.0171 (3)	0.0077 (2)	0.0086 (8)	0.0046 (6)	0.0168 (3)
O7	0.3406 (5)	0.5717 (4)	0.4336 (3)	0.0205 (7)	0.0168 (5)	0.0043 (2)	−0.0051 (11)	0.0030 (6)	−0.0012 (5)
O8	−0.2730 (5)	0.3691 (4)	0.3121 (4)	0.0113 (5)	0.0134 (4)	0.0138 (3)	0.0038 (8)	0.0109 (7)	0.0099 (5)
O9	0.0072 (5)	0.6256 (3)	0.3722 (2)	0.0261 (7)	0.0060 (2)	0.0060 (2)	0.0050 (7)	0.0110 (6)	0.0015 (3)
O10	0.1093 (6)	0.4185 (5)	0.4921 (2)	0.0371 (8)	0.0241 (6)	0.0047 (1)	0.0385 (9)	0.0147 (6)	0.0151 (3)
O11	0.1332 (5)	0.4245 (3)	0.0340 (2)	0.0301 (7)	0.0118 (3)	0.0038 (1)	−0.0156 (8)	0.0075 (5)	0.0028 (3)
O12	−0.2007 (4)	0.5482 (3)	0.1743 (3)	0.0126 (5)	0.0082 (2)	0.0085 (2)	0.0052 (6)	0.0021 (6)	0.0073 (3)
O13	0.2502 (5)	0.6374 (3)	0.2691 (2)	0.0207 (7)	0.0065 (2)	0.0056 (2)	−0.0077 (7)	−0.0016 (6)	0.0046 (3)
N1	0.2910 (4)	0.1540 (3)	0.7437 (2)	0.0119 (5)	0.0051 (2)	0.0022 (1)	0.0039 (6)	0.0040 (4)	0.0018 (3)
C1	0.0565 (7)	0.1549 (4)	0.1425 (3)	0.0206 (10)	0.0065 (3)	0.0050 (2)	0.0022 (10)	0.0038 (8)	0.0051 (4)
C2	0.2528 (6)	0.2914 (4)	0.1665 (3)	0.0125 (7)	0.0079 (3)	0.0031 (2)	0.0047 (8)	0.0041 (6)	0.0046 (3)
C3	0.0753 (6)	0.2573 (4)	0.2908 (3)	0.0173 (7)	0.0071 (3)	0.0049 (2)	0.0083 (8)	0.0103 (6)	0.0069 (3)
C4	−0.0682 (5)	0.3154 (3)	0.1485 (3)	0.0110 (6)	0.0049 (3)	0.0045 (2)	−0.0010 (7)	0.0022 (6)	0.0043 (3)
C5	0.4464 (6)	0.4492 (5)	0.2415 (3)	0.0122 (7)	0.0103 (4)	0.0035 (2)	0.0005 (9)	0.0042 (6)	0.0047 (4)
C6	0.3992 (6)	0.3256 (4)	0.3241 (3)	0.0127 (7)	0.0114 (4)	0.0046 (2)	0.0027 (9)	0.0036 (6)	0.0087 (4)
C7	0.3139 (6)	0.5094 (5)	0.3756 (3)	0.0136 (8)	0.0110 (5)	0.0037 (2)	−0.0011 (11)	0.0027 (7)	0.0041 (5)
C8	−0.1569 (6)	0.3841 (4)	0.3168 (4)	0.0139 (7)	0.0064 (3)	0.0064 (3)	0.0051 (9)	0.0077 (7)	0.0041 (5)
C9	0.0197 (6)	0.5447 (4)	0.3508 (3)	0.0145 (7)	0.0068 (3)	0.0036 (2)	0.0033 (9)	0.0063 (6)	0.0021 (4)
C10	0.0822 (6)	0.4119 (5)	0.4303 (3)	0.0191 (8)	0.0119 (4)	0.0043 (2)	0.0168 (9)	0.0097 (6)	0.0081 (4)
C11	0.1086 (6)	0.4342 (4)	0.0937 (3)	0.0172 (8)	0.0065 (3)	0.0037 (2)	−0.0073 (8)	0.0036 (6)	0.0029 (4)
C12	−0.1042 (6)	0.5107 (4)	0.1801 (3)	0.0136 (7)	0.0056 (3)	0.0038 (2)	0.0002 (8)	0.0017 (6)	0.0035 (4)
C13	0.1900 (6)	0.5645 (3)	0.2442 (3)	0.0148 (7)	0.0057 (3)	0.0032 (2)	−0.0010 (8)	0.0014 (6)	0.0035 (3)
C14	0.5224 (5)	0.0640 (4)	0.6808 (3)	0.0089 (6)	0.0050 (3)	0.0027 (2)	0.0025 (7)	0.0018 (5)	0.0003 (3)
C15	0.6304 (5)	0.1206 (4)	0.6722 (3)	0.0081 (6)	0.0069 (3)	0.0042 (2)	−0.0008 (8)	0.0012 (6)	0.0012 (4)
C16	0.7672 (6)	0.0988 (5)	0.6894 (4)	0.0089 (7)	0.0088 (4)	0.0063 (3)	0.0009 (9)	0.0014 (7)	0.0035 (5)
C17	0.7916 (6)	0.0212 (5)	0.7161 (4)	0.0126 (8)	0.0094 (4)	0.0047 (2)	0.0068 (10)	0.0014 (7)	0.0024 (5)
C18	0.6855 (6)	−0.0337 (4)	0.7234 (3)	0.0136 (7)	0.0084 (4)	0.0047 (2)	0.0093 (9)	0.0059 (7)	0.0041 (4)
C19	0.5470 (6)	−0.0139 (4)	0.7054 (3)	0.0131 (7)	0.0064 (3)	0.0041 (2)	0.0076 (8)	0.0041 (6)	0.0029 (4)
C20	0.3459 (5)	0.1763 (3)	0.6113 (3)	0.0076 (5)	0.0059 (3)	0.0026 (1)	0.0007 (7)	0.0018 (5)	0.0029 (3)
C21	0.3683 (6)	0.1373 (4)	0.5344 (3)	0.0119 (7)	0.0082 (4)	0.0029 (2)	0.0015 (8)	0.0038 (5)	0.0030 (4)
C22	0.3736 (6)	0.1977 (5)	0.4918 (3)	0.0135 (8)	0.0107 (4)	0.0039 (2)	0.0032 (10)	0.0031 (6)	0.0066 (4)
C23	0.3565 (6)	0.2968 (4)	0.5264 (3)	0.0116 (7)	0.0116 (4)	0.0048 (2)	0.0037 (9)	0.0034 (6)	0.0090 (4)
C24	0.3315 (6)	0.3347 (4)	0.6026 (3)	0.0156 (8)	0.0078 (3)	0.0043 (2)	0.0012 (9)	0.0010 (7)	0.0064 (4)
C25	0.3269 (6)	0.2743 (4)	0.6458 (3)	0.0120 (7)	0.0056 (3)	0.0036 (2)	0.0016 (8)	0.0016 (6)	0.0036 (3)
C26	0.2350 (5)	−0.0087 (4)	0.6073 (3)	0.0105 (6)	0.0046 (3)	0.0028 (2)	−0.0004 (7)	0.0031 (5)	0.0006 (3)
C27	0.0939 (6)	−0.0052 (4)	0.6113 (3)	0.0091 (6)	0.0076 (4)	0.0043 (2)	−0.0024 (8)	0.0019 (6)	0.0020 (4)
C28	0.0031 (7)	−0.0839 (5)	0.5649 (4)	0.0129 (8)	0.0096 (5)	0.0056 (3)	−0.0054 (10)	0.0020 (8)	0.0026 (6)
C29	0.0470 (7)	−0.1648 (5)	0.5133 (4)	0.0182 (10)	0.0078 (4)	0.0058 (3)	−0.0067 (11)	0.0035 (9)	0.0004 (6)
C30	0.1856 (8)	−0.1692 (5)	0.5095 (4)	0.0207 (11)	0.0071 (5)	0.0072 (4)	−0.0055 (12)	0.0050 (10)	−0.0051 (7)
C31	0.2823 (7)	−0.0886 (5)	0.5557 (4)	0.0170 (9)	0.0068 (4)	0.0055 (3)	−0.0025 (11)	0.0047 (9)	−0.0026 (6)
C32	0.4337 (5)	0.2596 (3)	0.8912 (2)	0.0094 (6)	0.0048 (2)	0.0026 (1)	0.0026 (6)	0.0026 (5)	0.0025 (3)
C33	0.4518 (6)	0.2883 (4)	0.9729 (3)	0.0142 (7)	0.0073 (3)	0.0027 (2)	0.0007 (9)	0.0032 (6)	0.0024 (4)
C34	0.5476 (6)	0.3654 (4)	1.0188 (3)	0.0138 (8)	0.0081 (4)	0.0030 (2)	0.0007 (10)	0.0010 (7)	0.0001 (5)
C35	0.6243 (6)	0.4156 (4)	0.9855 (3)	0.0133 (7)	0.0068 (3)	0.0039 (2)	0.0004 (9)	0.0021 (7)	0.0020 (4)
C36	0.6065 (6)	0.3869 (4)	0.9053 (3)	0.0128 (7)	0.0069 (3)	0.0038 (2)	−0.0029 (9)	0.0016 (6)	0.0023 (4)
C37	0.5124 (5)	0.3092 (4)	0.8580 (3)	0.0111 (6)	0.0057 (3)	0.0031 (2)	0.0001 (7)	0.0033 (5)	0.0026 (3)
C38	0.3612 (5)	0.0524 (4)	0.8474 (3)	0.0136 (6)	0.0055 (3)	0.0040 (2)	0.0062 (7)	0.0072 (5)	0.0048 (3)
C39	0.2680 (7)	−0.0312 (4)	0.8097 (4)	0.0193 (8)	0.0045 (3)	0.0069 (2)	0.0041 (8)	0.0107 (7)	0.0051 (4)
C40	0.3021 (7)	−0.1189 (4)	0.8159 (4)	0.0209 (10)	0.0075 (3)	0.0100 (3)	0.0090 (10)	0.0122 (9)	0.0104 (5)
C41	0.4267 (8)	−0.1238 (5)	0.8585 (4)	0.0269 (11)	0.0076 (4)	0.0096 (3)	0.0110 (11)	0.0154 (10)	0.0093 (5)
C42	0.5235 (8)	−0.0422 (4)	0.8951 (4)	0.0261 (10)	0.0100 (4)	0.0071 (3)	0.0185 (24)	0.0097 (9)	0.0089 (5)
C43	0.4900 (7)	0.0495 (4)	0.8892 (3)	0.0176 (8)	0.0090 (3)	0.0047 (2)	0.0018 (9)	0.0041 (7)	0.0071 (4)
C44	0.1474 (5)	0.1846 (3)	0.8636 (2)	0.0094 (5)	0.0043 (2)	0.0024 (1)	0.0003 (6)	0.0023 (5)	0.0016 (3)
C45	0.1088 (6)	0.1490 (4)	0.9186 (3)	0.0135 (6)	0.0063 (3)	0.0038 (2)	0.0044 (8)	0.0066 (5)	0.0046 (3)
C46	−0.0164 (6)	0.1723 (4)	0.9450 (3)	0.0153 (7)	0.0068 (3)	0.0042 (2)	0.0042 (8)	0.0076 (6)	0.0042 (4)
C47	−0.1005 (6)	0.2297 (4)	0.9173 (3)	0.0113 (6)	0.0070 (3)	0.0044 (2)	0.0019 (8)	0.0053 (6)	0.0027 (4)
C48	−0.0624 (6)	0.2668 (4)	0.8637 (3)	0.0115 (7)	0.0091 (4)	0.0050 (2)	0.0064 (9)	0.0050 (6)	0.0058 (4)
C49	0.0615 (5)	0.2431 (4)	0.8354 (3)	0.0108 (6)	0.0057 (3)	0.0039 (2)	0.0040 (7)	0.0032 (6)	0.0041 (3)

[a] The form of the anisotropic thermal parameter is $\exp[-(B_{11}h^2 + B_{22}k^2 + B_{33}l^2 + B_{12}hk + B_{13}hl + B_{23}kl)]$.

An ORTEP drawing which shows the atom numbering scheme for the [CoRu$_3$(CO)$_{13}$]$^-$ anion is shown in Figure 1 and a stereoview of the anion is given in Figure 2. Final positional and thermal parameters are listed in Table II. Relevant bond distances and bond angles are set out in Tables III and IV. A listing of the observed and calculated structure factors is given as supplementary material.

Results

General Synthetic Approach. As previously described,[1] our approach to the synthesis of a particular tetranuclear cluster

Table III. Selected Bond Distances (A) in [PPN][CoRu₃(CO)₁₃]

Ru1-Ru2	2.835 (1)	C1-O1	1.131 (5)		
Ru1-Ru3	2.828 (1)	C2-O2	1.170 (4)		
Ru2-Ru3	2.824 (1)	C3-O3	1.154 (4)		
Ru1-Co	2.631 (1)	C4-O4	1.158 (4)		
Ru2-Co	2.612 (1)	C5-O5	1.135 (5)		
Ru3-Co	2.611 (1)	C6-O6	1.129 (5)		
Co-C1	1.743 (5)	C7-O7	1.138 (5)		
Co-C2	1.856 (4)	C8-O8	1.134 (5)		
Co-C3	1.861 (4)	C9-O9	1.136 (5)		
Co-C4	1.850 (4)	C10-O10	1.111 (5)		
Ru1-C4	2.151 (4)	C11-O11	1.139 (5)		
Ru1-C5	1.902 (4)	C12-O12	1.117 (4)		
Ru1-C6	1.885 (5)	C13-O13	1.120 (4)		
Ru1-C7	1.904 (5)				
Ru2-C3	2.170 (4)	N-P1	1.579 (3)		
Ru2-C8	1.876 (5)	N-P2	1.578 (3)		
Ru2-C9	1.908 (5)	P1-C14	1.810 (4)		
Ru2-C10	1.921 (5)	P1-C20	1.797 (4)		
Ru3-C4	2.172 (4)	P1-C26	1.795 (3)		
Ru3-C11	1.889 (4)	P2-C32	1.784 (4)		
Ru3-C12	1.904 (5)	P2-C38	1.804 (4)		
Ru3-C13	1.919 (4)	P2-C44	1.792 (3)		

Table IV. Selected Bond Angles (Deg) in [PPN][CoRu₃(CO)₁₃]

Ru1-Ru2-Ru3	60.0 (1)	Ru3-Ru2-C9	73.0 (1)
Ru1-Ru3-Ru2	60.2 (1)	Ru3-Ru2-C10	157.8 (2)
Ru2-Ru1-Ru3	59.8 (1)	Co-Ru2-C8	101.9 (1)
Ru1-Co-Ru2	65.5 (1)	Co-Ru2-C9	130.2 (1)
Ru1-Co-Ru3	65.3 (1)	Co-Ru2-C10	127.9 (1)
Ru2-Co-Ru3	65.5 (1)	Ru1-Ru3-C11	106.8 (1)
Co-Ru1-Ru2	57.0 (1)	Ru1-Ru3-C12	154.2 (1)
Co-Ru1-Ru3	57.0 (1)	Ru1-Ru3-C13	70.5 (1)
Co-Ru2-Ru3	57.3 (1)	Ru2-Ru3-C11	159.3 (1)
Co-Ru2-Ru1	57.6 (1)	Ru2-Ru3-C12	99.1 (1)
Co-Ru3-Ru1	57.7 (1)	Ru2-Ru3-C13	96.4 (1)
Co-Ru3-Ru2	57.3 (1)	Co-Ru3-C11	102.5 (1)
Co-C2-O2	140.9 (4)	Co-Ru3-C12	126.5 (1)
Ru1-C2-O2	137.4 (3)	Co-Ru3-C13	128.1 (1)
Co-C3-O3	143.2 (4)	Ru1-Co-C1	138.4 (2)
Ru2-C3-O3	136.4 (3)	Ru2-Co-C1	143.2 (2)
Co-C4-O4	142.6 (3)	Ru3-Co-C1	142.5 (2)
Ru3-C4-O4	136.9 (3)	Ru3-Ru1-C2	72.1 (1)
Ru2-Ru1-C5	156.1 (1)	Ru1-Ru2-C3	76.1 (1)
Ru2-Ru1-C6	105.3 (1)	Ru2-Ru3-C4	75.4 (1)
Ru2-Ru1-C7	73.1 (1)	Co-C1-O1	179.1 (5)
Ru3-Ru1-C5	101.7 (1)	Ru1-C5-O5	178.4 (4)
Ru3-Ru1-C6	154.6 (1)	Ru1-C6-O6	178.4 (5)
Ru3-Ru1-C7	101.0 (2)	Ru1-C7-O7	171.6 (4)
Co-Ru1-C5	128.2 (1)	Ru2-C8-O8	179.3 (5)
Co-Ru1-C6	97.9 (2)	Ru2-C9-O9	173.4 (4)
Co-Ru1-C7	130.0 (1)	Ru2-C10-O10	176.5 (5)
Ru1-Ru2-C8	158.3 (2)	Ru3-C11-O11	178.9 (5)
Ru1-Ru2-C9	96.7 (1)	Ru3-C12-O12	178.2 (4)
Ru1-Ru2-C10	102.8 (1)	Ru3-C13-O13	169.6 (4)
Ru3-Ru2-C8	104.4 (2)	P1-N-P2	140.0 (2)

Figure 1. Structure of the [CoRu₃(CO)₁₃]⁻ anion showing the atom numbering scheme. Thermal ellipsoids are drawn at the 20% probability level. The terminal carbonyl (C₁, O₁) attached to Co is omitted for clarity (see Figure 2).

is to add an appropriate carbonylmetalate to an appropriate closed metal carbonyl trimer. For example, [CoRu₃(CO)₁₃]⁻ is synthesized by the addition of [Co(CO)₄]⁻ to Ru₃(CO)₁₂, eq 2. This particular anion can either be isolated as its PPN⁺

$$Ru_3(CO)_{12} + [Co(CO)_4]^- \rightarrow [CoRu_3(CO)_{13}]^- + CO \quad (2)$$

salt or protonated to yield HCoRu₃(CO)₁₃. The synthesis of each of the hydride clusters described below was carried out

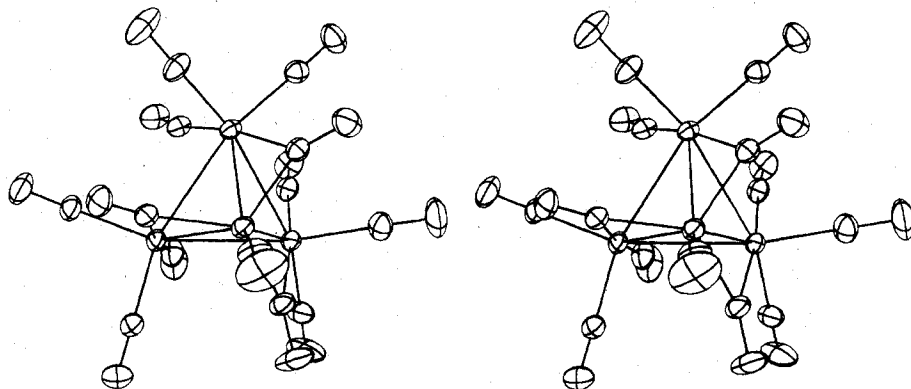in essentially the same manner. A THF solution of the trimer was added dropwise to a freshly prepared, refluxing THF solution of K[Co(CO)₄] under an N₂ atmosphere. After heating of the mixture, the THF was removed by evaporation under vacuum. The resultant residue was then acidified with H₃PO₄ and extracted into hexane or benzene. Extract solutions were dried over anhydrous MgSO₄, concentrated, and then chromatographed on silica gel. Specific details concerning reaction times, yields, and chromatography are given in the Experimental Section.

The experimental procedure for the synthesis of each of the anionic clusters was similar. A dried, deoxygenated THF solution of [PPN][Co(CO)₄] and the appropriate trimer was refluxed under an N₂ atmosphere. The THF was then removed by evaporation under vacuum and the resultant solid dissolved in the minimum amount of dried and deoxygenated Et₂O. Any unreacted [PPN][Co(CO)₄] is insoluble in Et₂O and remains behind as a tan residue. The cluster was then recrystallized by slow diffusion of hexane into the Et₂O solution.

Of the various spectroscopic techniques used to identify the products of the reactions, the most useful were infrared and mass spectrometry. Previously described clusters were iden-


Figure 2. Stereoscopic view of [CoRu₃(CO)₁₃]⁻.

Table V. Infrared and Electronic Absorption Spectral Data[a]

cluster	color	λ_{max}, nm	ν_{CO}(terminal), cm^{-1}	ν_{CO}(bridging), cm^{-1}
[PPN][CoFe$_3$(CO)$_{13}$]	black	585	2074 w, 2004 vs, 1971 m, 1930 m, sh	1816 m, br
[PPN][CoFe$_2$Ru(CO)$_{13}$]	brown	406	2074 w, 2030 s, 2008 vs, 1997 s, sh, 1950 m, sh	1826 w, sh, 1796 m, br
[PPN][CoFeRu$_2$(CO)$_{13}$]	red-brown	404	2072 w, 2028 s, 2008 vs, 1195 s, sh, 1950 m, sh	1826 w, sh, 1795 m, br
[PPN][CoRu$_3$(CO)$_{13}$]	red	390	2072 w, 2024 vs, 1992 m	1823 w, sh, 1794 m, br
HCoRu$_3$(CO)$_{13}$	red	550 sh, 348	2109 w, 2058 w, 2013 s, 2061 vs, 2054 vs, 2034 m, 2024 m, 2017 m, 1971 w	1990 w, 1865 m
HCoRu$_2$Os(CO)$_{13}$	orange	544 sh, 352	2111 w, 2076 s, 2056 vs, 2034 m, 2028 m, 2018 m	1907 w, 1862 m
HCoRuOs$_2$(CO)$_{13}$	orange	520 sh	2122 w, 2078 s, 2056 vs, 2035 m, 2030 m, 2018 w, 1996 s	1903 w
HCoOs$_3$(CO)$_{13}$	yellow		2114 vw, 2080 s, 2058 vs, 2037 m, 2030 m, 2016 w, 1997 w	1899 w, 1858 m

[a] Data taken from CH$_2$Cl$_2$ solutions of the anionic clusters and hexane solutions of the neutral clusters.

tified mainly by comparison to their reported infrared data. Infrared, electronic absorption, and ^{1}H NMR data for the new clusters prepared in this work are set out in Tables V and VI, respectively. Mass spectral data are summarized in Table C (supplementary material).

Preparation of HCoRu$_3$(CO)$_{13}$. The synthesis of HCoRu$_3$(CO)$_{13}$ was accomplished by allowing K[Co(CO)$_4$] to react with Ru$_3$(CO)$_{12}$ in refluxing THF solution for 2.5 h followed by protonation with H$_3$PO$_4$, eq 3. This reaction produced the

$$[Co(CO)_4]^- + Ru_3(CO)_{12} \xrightarrow[THF]{\Delta} [CoRu_3(CO)_{13}]^- \xrightarrow{H_3PO_4}$$
$$HCoRu_3(CO)_{13} \quad (3)$$
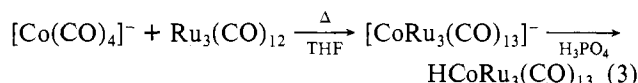
desired HCoRu$_3$(CO)$_{13}$ in 63% yield along with a trace of H$_2$Ru$_4$(CO)$_{13}$ as the only other product. A significant amount of Ru$_3$(CO)$_{12}$ was also recovered. The new cluster HCoRu$_3$(CO)$_{13}$ was characterized by its spectral data and by chemical analysis. Solid samples of HCoRu$_3$(CO)$_{13}$ decompose over a period of weeks when stored under N$_2$ at room temperature. Decomposition is accelerated upon exposure of samples to air. Even in dried, degassed isooctane solution, decomposition sets in within minutes and is apparently complete within 2–3 days. The only decomposition product positively identified is Ru$_3$(CO)$_{12}$. Decomposition is complete within minutes upon exposure of solutions to CO, giving Ru$_3$(CO)$_{12}$, Ru(CO)$_5$, and Co$_2$(CO)$_8$ as products.[10]

Preparation of [PPN][CoRu$_3$(CO)$_{13}$]. The [CoRu$_3$(CO)$_{13}$]$^-$ anion was obtained in 64% yield as its PPN salt by allowing [PPN][Co(CO)$_4$] to react with Ru$_3$(CO)$_{12}$ in refluxing THF solution for 2.5 h followed by recrystallization from Et$_2$O/hexane.[11] Unlike HCoRu$_3$(CO)$_{13}$, [PPN][CoRu$_3$(CO)$_{13}$] appears to be indefinitely stable in air both in the solid state and in solution. All attempts to convert [PPN][CoRu$_3$(CO)$_{13}$] into HCoRu$_3$(CO)$_{13}$ by protonation with H$_3$PO$_4$ failed.

Preparation of HCoRu$_2$Os(CO)$_{13}$ and HCoRuOs$_2$(CO)$_{13}$. To synthesize HCoRu$_2$Os(CO)$_{13}$ and HCoRuOs$_2$(CO)$_{13}$, we allowed K[Co(CO)$_4$] to react with the Ru$_3$-, Ru$_2$Os-, RuOs$_2$-, and Os$_3$(CO)$_{12}$ trimer mixture[5,8] in refluxing THF for 3.5 h followed by protonation with H$_3$PO$_4$, eq 4. This reaction also

$$Ru_2Os(CO)_{12} + RuOs_2(CO)_{12} + [Co(CO)_4]^- \xrightarrow[THF]{\Delta, 3.5 \text{ h}}$$
$$\xrightarrow{H_3PO_4} \underset{38\%}{HCoRu_2Os(CO)_{13}} + \underset{25\%}{HCoRuOs_2(CO)_{13}} \quad (4)$$
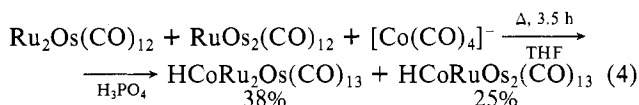
produced a small amount of HCoRu$_3$(CO)$_{13}$, and a significant amount of the trimer mixture was recovered. The stabilities of HCoRu$_2$Os(CO)$_{13}$ and HCoRuOs$_2$(CO)$_{13}$ parallel that of HCoRu$_3$(CO)$_{13}$, described above. These clusters were principally characterized by their mass spectra, Table C, which showed parent ions at the correct m/e values with the expected

Table VI. ^{1}H NMR Spectral Data[a]

cluster	δ	cluster	δ
HCoRu$_3$(CO)$_{13}$	−17.8	H$_2$FeRu$_3$(CO)$_{13}$	−18.4[b]
HCoRu$_2$Os(CO)$_{13}$	−18.5	H$_2$FeRu$_2$Os(CO)$_{13}$	−19.1[b,c]
HCoRuOs$_2$(CO)$_{13}$	−19.1	H$_2$FeRuOs$_2$(CO)$_{13}$	−19.7[b,c]

[a] Measured in CDCl$_3$ solutions. [b] References 24 and 25. [c] Average of three different hydrogen environments: H$_2$FeRu$_2$Os(CO)$_{13}$ (−18.97, −19.11, −19.19), H$_2$FeRuOs$_2$(CO)$_{13}$ (−19.55, −19.67, −19.82).

isotopic distributions and also fragment ions corresponding to loss of each of the 13 carbonyls. Repeated attempts at obtaining satisfactory elemental analyses failed. We subsequently discovered that silica gel enhances the rate of decomposition of these clusters and may explain why repeated chromatography on SiO$_2$ did not yield pure products.

Attempted Preparation of HCoOs$_3$(CO)$_{13}$. We expected that HCoOs$_3$(CO)$_{13}$ would result from the addition of K[Co(CO)$_4$] to Os$_3$(CO)$_{12}$ followed by protonation. However, we were unable to isolate any of the desired cluster following attempts to synthesize it directly, even though the reaction conditions were varied considerably. Only Os$_3$(CO)$_{12}$, H$_2$Os$_4$(CO)$_{13}$, H$_4$Os$_4$(CO)$_{12}$, and Co$_4$(CO)$_{12}$ were isolated following the usual chromatographic separation of the protonated reaction mixtures. In a single experiment in which the reaction mixture resulting from the addition of K[Co(CO)$_4$] to the Ru$_3$-, Ru$_2$Os-, RuOs$_2$-, and Os$_3$(CO)$_{12}$ trimer mixture was separated by ultra-high-speed liquid chromatography,[12] we did isolate a very small amount of a yellow solid which eluted after HCoRuOs$_2$(CO)$_{13}$. This material was shown to be HCoOs$_3$(CO)$_{13}$ by its mass spectrum, Table C. IR data for the compound are given in Table V, but insufficient material could be isolated for further characterization. Apparently HCoOs$_3$(CO)$_{13}$ is formed in the attempted syntheses, but it must be inherently unstable and like HCoRuOs$_2$(CO)$_{13}$ and HCoRu$_2$Os(CO)$_{13}$ its decomposition may be accelerated by SiO$_2$.

Preparation of [PPN][CoFe$_3$(CO)$_{13}$]. The anion [CoFe$_3$(CO)$_{12}$]$^-$ has been mentioned by Chini and Heaton[2] but no preparative details were given. In our hands, black air-stable crystals of [PPN][CoFe$_3$(CO)$_{13}$] resulted in 18% yield from the reaction of [PPN][Co(CO)$_4$] with Fe$_3$(CO)$_{12}$ in THF solution at room temperature, eq 5.

$$[Co(CO)_4]^- + Fe_3(CO)_{12} \xrightarrow[THF]{25 \text{ °C, 22 h}}$$
$$[CoFe_3(CO)_{12}]^- \text{ (18%)} \quad (5)$$
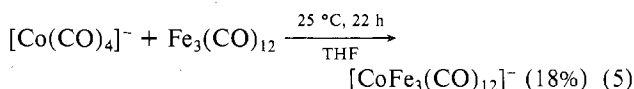
Attempted Preparation of HCoFe$_3$(CO)$_{13}$. Although the [CoFe$_3$(CO)$_{13}$]$^-$ anion appears to be quite stable, we have not been able to prepare HCoFe$_3$(CO)$_{13}$. We attempted to synthesize HCoFe$_3$(CO)$_{13}$ by allowing K[Co(CO)$_4$] to react with Fe$_3$(CO)$_{12}$ followed by protonation with H$_3$PO$_4$. A rapid green

(10) Fox, J. R.; Gladfelter, W. L.; Geoffroy, G. L., submitted for publication in *Inorg. Chem.*
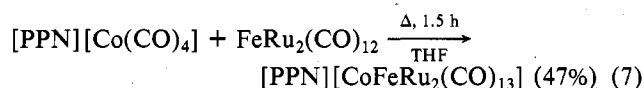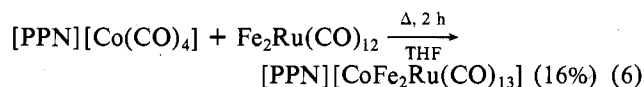
(11) This compound has been independently prepared by R. Bau and L. Garlaschelli by an exactly analogous procedure (R. Bau, private communication).

(12) This separation was conducted on a Waters Associates Prep LC/System 500 using SiO$_2$ columns with hexane as the eluting solvent at a flow rate of 100 mL/min.

to red color change ensued when these reactants were refluxed in THF for 3 h, indicating that the desired reaction occurred (see above). However, only $Fe_3(CO)_{12}$, $HCo_3Fe(CO)_{12}$,[13] and $Co_4(CO)_{12}$ were isolated from the acidified solution. The same product mixture resulted when the reaction mixture was maintained at 40 °C for 3 h instead of at reflux as above and when $K[Co(CO)_4]$ was added to $Fe_3(CO)_{12}$, the reverse of the usual order of reagent addition. Attempts to form $HCoFe_3$-$(CO)_{13}$ via protonation of $[PPN][CoFe_3(CO)_{13}]$ with H_3PO_4 also failed.

Attempted Preparation of $HCoFe_2Ru(CO)_{13}$ and $HCoFe$-$Ru_2(CO)_{13}$. We attempted to prepare the unknown HCo-$Fe_2Ru(CO)_{13}$ and $HCoFeRu_2(CO)_{13}$ clusters by the addition of $K[Co(CO)_4]$ to $Fe_2Ru(CO)_{12}$ and $FeRu_2(CO)_{12}$ but without success. Reaction of $K[Co(CO)_4]$ with $Fe_2Ru(CO)_{12}$ gave $Co_4(CO)_{12}$ and $HCo_3Ru(CO)_{12}$[14] as the principal products. Reaction of $K[Co(CO)_4]$ with $FeRu_2(CO)_{12}$ gave $Ru_3(CO)_{12}$, $Co_4(CO)_{12}$, and $HCoRu_3(CO)_{13}$.

Preparation of $[PPN][CoFe_2Ru(CO)_{13}]$ and $[PPN][CoFe$-$Ru_2(CO)_{13}]$. Impure samples of these clusters were obtained from the respective reactions of $[PPN][Co(CO)_4]$ with Fe_2-$Ru(CO)_{12}$ and $FeRu_2(CO)_{12}$, eq 6 and 7. The crude reaction

$$[PPN][Co(CO)_4] + Fe_2Ru(CO)_{12} \xrightarrow[\text{THF}]{\Delta,\ 2\ h}$$
$$[PPN][CoFe_2Ru(CO)_{13}]\ (16\%)\ (6)$$

$$[PPN][Co(CO)_4] + FeRu_2(CO)_{12} \xrightarrow[\text{THF}]{\Delta,\ 1.5\ h}$$
$$[PPN][CoFeRu_2(CO)_{13}]\ (47\%)\ (7)$$

products were recrystallized from Et_2O/hexane to give the yields of crystalline material shown above. These clusters were principally characterized by infrared spectroscopy and by comparison of their spectral data to the other clusters described herein. Repeated attempts to obtain satisfactory elemental analyses for these compounds failed, but as illustrated by the data given in the Experimental Section, Fe and Ru were present in each case and in near the expected ratio for $[PP$-$N][CoFeRu_2(CO)_{13}]$. Anionic clusters such as these do not exhibit well-behaved chromatographic properties, and we have been unable to purify them by chromatography or by fractional crystallization.

Crystal Structure of $[PPN][CoRu_3(CO)_{13}]$. The crystal structure of $[PPN][CoRu_3(CO)_{13}]$ shows that the compound consists of discrete cations and anions with the latter having a tetrahedral arrangement of metal atoms as shown in Figure 1. The three Ru–Ru distances are nearly equal (2.824, 2.828, 2.835 Å) as are the three Co–Ru distances (2.611, 2.612, 2.631 Å). Each Ru bears three terminal carbonyl ligands, the Co has one terminal carbonyl, and three carbonyls bridge the three Co–Ru bonds. The latter appear to be full-bridging carbonyls, rather than semibridging, as evidenced by the near-equivalence of the Co–C–O (140–142°) and Ru–C–O (141–143°) bond angles. In the isoelectronic $H_2FeRu_3(CO)_{13}$ cluster which possesses two semibridging carbonyls across Fe–Ru bonds, the Ru–C–O angles (120–124°) and the Fe–C–O angles (145–156°) differ markedly.[15] Furthermore, the $Ru-C_{bridging}$ bond lengths (2.15–2.17 Å) in $[PPN][CoRu_3(CO)_{13}]$ are significantly shorter than those in $H_2FeRu_3(CO)_{13}$ (2.23–2.32 Å), even though the Co–Ru (2.611–2.631 Å) and the Fe–Ru (2.619–2.700 Å) bond lengths in the two clusters are comparable.

Application of the usual simple electron-counting schemes shows that this cluster has the requisite 60 valence electrons expected for a tetrahedral structure.[16] Furthermore, since the three bridging carbonyls appear to be equally shared by the three Ru's and the Co, the negative charge of the cluster should be localized on Co in order to give this metal the required 18 electrons. The PPN cation is bent (PPN = 140.0°) and shows no unusual structural features.

This is the only tetranuclear cluster which has been shown to possess three bridging CO's all attached to the same metal atom. The highest symmetry that such a cluster could possess is C_{3v} if each of the three bridging CO's and the metal atoms which they bridge were to lie in one of the three mirror planes. The terminal carbonyl ligands in such a structure would likely be disposed so that each would be approximately trans to one of the metal–metal bonds. However, the $[CoRu_3(CO)_{13}]^-$ anion does not adopt this structure. Instead, as illustrated in Figure 1, the three bridging CO's are arranged in a staggered fashion about the Co atom and each lies nearly within one of the planes defining the three $CoRu_2$ faces; the $C_{bridging}$ atoms deviate from these planes by 0.23 Å (C_2), 0.09 Å (C_3), and 0.10 Å (C_4). The three $Ru(CO)_3$ units are rotated so that the terminal carbonyls are not trans to the M–M bonds but rather the carbonyls are arranged in positions that apparently minimize steric interactions. One terminal carbonyl on each Ru actually lies above the Ru_3 plane. Even so, the cluster still possesses a pseudo-C_3 rotation axis and thus approximates C_3 symmetry.

Further inspection of the structure of $[CoRu_3(CO)_{13}]^-$ shows that the anion is chiral. This is best illustrated by A and B

A   B
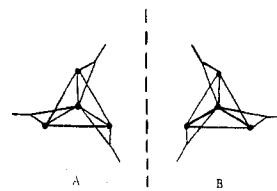
which show the metal framework and the disposition of the three bridging CO's. The enantiomer on the left, A, which is the one depicted in Figures 1 and 2, is clearly not superimposable on its mirror image, B. Because of the centrosymmetric nature of the crystal, space group $P\bar{1}$, both enantiomers are present in the unit cell. The interesting possibility is raised that these enantiomers may be separable, although cluster fluxional processes could lead to ready racemization. The variable-temperature ^{13}C NMR properties of this cluster are under study and will be the subject of a future report.

Discussion

Synthesis. The basic reaction approach employed in this study for the synthesis of tetranuclear clusters is the addition of a carbonylmetalate to a closed metal carbonyl trimer. The reactions examined and the resultant products are summarized in Scheme I. The principal products are indicated with an asterisk, and specific yields are given in the Experimental Section. Tetranuclear clusters with the desired metal framework were produced when $[Co(CO)_4]^-$ was allowed to react with $Fe_3(CO)_{12}$, $Fe_2Ru(CO)_{12}$, $FeRu_2(CO)_{12}$, $Ru_3(C$-$O)_{12}$, $Ru_2Os(CO)_{12}$, and $RuOs_2(CO)_{12}$. Several of the clusters apparently decompose following protonation and could only be isolated as anions.

The mechanism by which a tetrahedral cluster results from the addition of a carbonylmetalate to a metal trimer is obviously complex and has been discussed in detail in previous publications.[1,17] Basically, we suggest that in the examples discussed herein, the nucleophilic $[Co(CO)_4]^-$ initially attacks the electropositive carbon of a bound carbon monoxide. Elimination of carbon monoxide with concomitant metal–metal
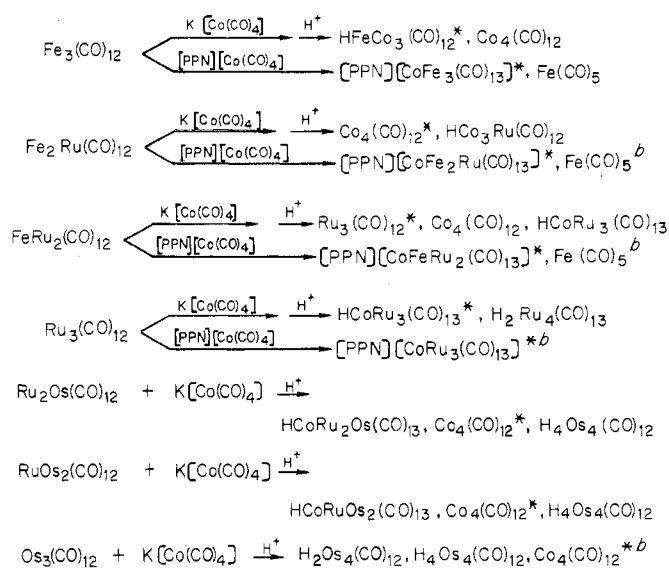
(13) Chini, P.; Colli, L.; Peraldo, M. *Gazz. Chim. Ital.* **1960**, *90*, 1005.
(14) Mays, M. J.; Simpson, R. N. F. *J. Chem. Soc. A* **1968**, 1444.
(15) Gilmore, C. J.; Woodward, P. *J. Chem. Soc. A* **1971**, 3453.

(16) Wade, K. *Adv. Inorg. Chem. Radiochem.* **1976**, *18*, 1.
(17) Knight, J.; Mays, M. J. *J. Chem. Soc., Dalton Trans.* **1972**, 1022.

Scheme I[a]

Fe$_3$(CO)$_{12}$

K [Co(CO)$_4$] → H$^+$ → HFeCo$_3$(CO)$_{12}$*, Co$_4$(CO)$_{12}$

[PPN][Co(CO)$_4$] → [PPN][CoFe$_3$(CO)$_{13}$]*, Fe(CO)$_5$

Fe$_2$Ru(CO)$_{12}$

K [Co(CO)$_4$] → H$^+$ → Co$_4$(CO)$_{12}$*, HCo$_3$Ru(CO)$_{12}$

[PPN][Co(CO)$_4$] → [PPN][CoFe$_2$Ru(CO)$_{13}$]*, Fe(CO)$_5$[b]

FeRu$_2$(CO)$_{12}$

K [Co(CO)$_4$] → H$^+$ → Ru$_3$(CO)$_{12}$*, Co$_4$(CO)$_{12}$, HCoRu$_3$(CO)$_{13}$

[PPN][Co(CO)$_4$] → [PPN][CoFeRu$_2$(CO)$_{13}$]*, Fe(CO)$_5$[b]

Ru$_3$(CO)$_{12}$

K [Co(CO)$_4$] → H$^+$ → HCoRu$_3$(CO)$_{13}$*, H$_2$Ru$_4$(CO)$_{13}$

[PPN][Co(CO)$_4$] → [PPN][CoRu$_3$(CO)$_{13}$]*[b]

Ru$_2$Os(CO)$_{12}$ + K[Co(CO)$_4$] →H$^+$→

HCoRu$_2$Os(CO)$_{13}$, Co$_4$(CO)$_{12}$*, H$_4$Os$_4$(CO)$_{12}$

RuOs$_2$(CO)$_{12}$ + K[Co(CO)$_4$] →H$^+$→

HCoRuOs$_2$(CO)$_{13}$, Co$_4$(CO)$_{12}$*, H$_4$Os$_4$(CO)$_{12}$

Os$_3$(CO)$_{12}$ + K[Co(CO)$_4$] →H$^+$→ H$_2$Os$_4$(CO)$_{12}$, H$_4$Os$_4$(CO)$_{12}$, Co$_4$(CO)$_{12}$*[b]

[a] Asterisk denotes principal product. [b] Plus unidentified products.

bond formation would then yield a tetramer with structure **1**. Subsequent closure by nucleophilic attack at the other metal atoms with consequent elimination of carbon monoxide would lead through **2** to a closed tetrahedral cluster **3**.

M | M—M \M/

1

M / M-▲-M \M/

2

M / M-▲-M \M/

3

In the mechanism described above, it is apparent that a crucial step involves formation of the first metal–metal bond. Two factors appear important in influencing the probability of occurrence of this first addition. The initial attack on the carbonyl carbon should depend on the nucleophilicity of the carbonylmetalate. In a comparative study of the relative nucleophilicities of a series of carbonylmetalates, [Co(CO)$_4$]$^-$ was determined to be the least nucleophilic of those examined.[18] However, the successful synthesis of the clusters reported herein clearly indicates that the low nucleophilicity of [Co(CO)$_4$]$^-$ is not a limiting factor in syntheses of this type.

The second important factor which influences the probability of success in using this synthetic approach is the metal–carbonyl bond strength of the trimer. In forming the first metal–metal bond to reach structure **1**, one trimer-CO bond must be replaced by a metal–metal bond (M–M'). The stronger the M–CO bond of the trimer is, the more difficult it will be to substitute CO by [Co(CO)$_4$]$^-$. Microcalorimetric measurements have given the ordering of the M–CO bond strengths in the M$_3$(CO)$_{12}$ trimers as Os–CO > Ru–CO > Fe–CO.[19,20] The relative strength of the Os–CO bond may account for our inability to produce isolable quantities of HCoOs$_3$(CO)$_{13}$ using this synthetic approach. As noted previously,[1] it appears that the order of trimer reactivity toward [M(CO)$_4$]$^{n-}$ (M = Fe, Co) addition is Fe$_3$(CO)$_{12}$ > Ru$_3$(CO)$_{12}$ > Os$_3$(CO)$_{12}$, in accord with the M–CO bond strengths.

A further complicating feature in syntheses which employ carbonylmetalates is the tendency of the carbonylmetalate to reduce and fragment the metal carbonyl trimer.[1,21] In all the
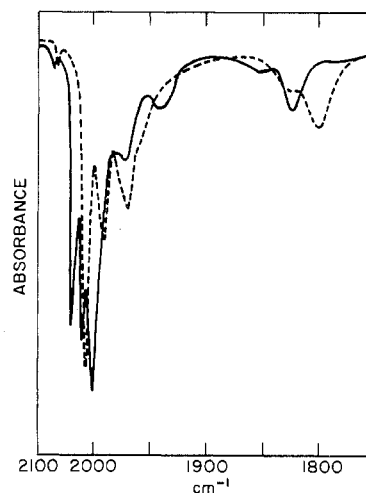

Figure 3. Comparison of the infrared spectra of [PPN][CoRu$_3$(CO)$_{13}$] (—) and [PPN][HFeRu$_3$(CO)$_{13}$] (- - -) in THF solution.

reactions which employed Fe$_3$(CO)$_{12}$, Fe$_2$Ru(CO)$_{12}$, and FeRu$_2$(CO)$_{12}$, some Fe(CO)$_5$ was detected during workup of the reaction mixtures. The latter likely arises through fragmentation to give Fe(CO)$_4$ which subsequently scavenges CO released during the course of the reaction. Such fragmentation and resultant scrambling of the metals in the syntheses employing Fe$_2$Ru(CO)$_{12}$ and FeRu$_2$(CO)$_{12}$ may account for our inability to obtain analytically pure samples of [PPN][CoFeRu$_2$(CO)$_{13}$] and [PPN][CoFe$_2$Ru(CO)$_{13}$]. Chini[2] has written the balanced eq 8 for his independent preparation of [CoFe$_3$(CO)$_{13}$]$^-$. If we assume that the given stoichiometry is accurate, it implies that this and perhaps the other syntheses reported herein are more complex in mechanism than we have assumed.

$$2Fe_3(CO)_{12} + [Co(CO)_4]^- \xrightarrow[THF]{25\,°C}$$

$$[CoFe_3(CO)_{13}]^- + 3Fe(CO)_5 \quad (8)$$
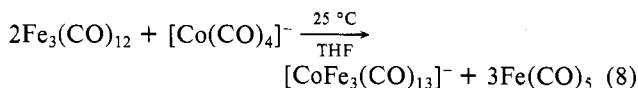
Characterization. 1. [PPN][CoRu$_3$(CO)$_{13}$]. This cluster was unambiguously characterized by determining its structure by X-ray diffraction. The details of the structure are discussed earlier in this report with the important features shown in Figures 1 and 2. The IR spectrum of the cluster is shown in Figure 3, and the IR data are summarized in Table V. As expected on the basis of its structure, the anion shows both terminal and bridging ν_{CO} bands. Two bands at 1823 (w) and 1794 (m) cm^{-1} are present in the bridging ν_{CO} region, consistent with the near C_3 symmetry of the cluster; two bands of A and E symmetries are expected, with the usual pattern of the higher energy A band being less intense than the lower energy E band.[22]

2. [PPN][CoFe$_3$(CO)$_{13}$], [PPN][CoFe$_2$Ru(CO)$_{13}$], and [PPN][CoFeRu$_2$(CO)$_{13}$]. These clusters were characterized by their spectral data, Table V, and by chemical analyses, although neither of the latter two clusters could be obtained pure. Consideration of the possible structures of these clusters raises an interesting question. Do they adopt structures similar to that of [CoRu$_3$(CO)$_{13}$]$^-$ or rather do they resemble the structure of [HFeRu$_3$(CO)$_{13}$]$^-$ with which they also are isoelectronic and which has the structure shown in **4**[23] with *two* bridging CO's? The latter is structurally related to H$_2$FeRu$_3$(CO)$_{13}$[15] from which it can be derived by deprotonation with KH.[23] [PPN][CoFeRu$_2$(CO)$_{13}$] illustrates this dilemma
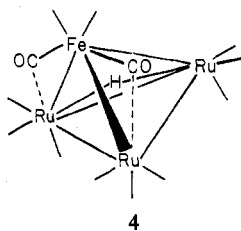
(18) King, R. B. *Acc. Chem. Res.* **1970**, *3*, 417.
(19) Conner, J. A.; Skinner, H. A.; Virmani, Y. *J. Chem. Soc., Faraday Trans. 1*, **1972**, *68*, 1754.
(20) Conner, J. A. *Top. Curr. Chem.* **1977**, *71*, 71.

(21) The reduction potential order is Fe$_3$(CO)$_{12}$ < Ru$_3$(CO)$_{12}$ < Os$_3$(CO)$_{12}$: Bond, A. M.; Dawson, P. A.; Peake, B. M.; Robinson, B. H.; Simpson, J. *Inorg. Chem.* **1977**, *16*, 2199.
(22) Braterman, P. S. "Metal Carbonyl Spectra"; Academic Press: London, 1975; p 44.

4

particularly well since it can be viewed as deriving from $[CoRu_3(CO)_{13}]^-$ by substitution of Fe for one Ru or alternately from $[HFeRu_3(CO)_{13}]^-$ by replacement of an HRu unit by Co. Unfortunately, IR spectroscopy does not allow a differentiation between these two basic structures since the IR spectra of $[CoRu_3(CO)_{13}]^-$ and $[HFeRu_3(CO)_{13}]^-$ are not sufficiently different, Figure 3. The question of the structures of these three anionic clusters will have to be left unanswered until resolution by X-ray diffraction or perhaps by careful ^{13}C NMR studies.

$HCoRu_3(CO)_{13}$, $HCoRu_2Os(CO)_{13}$, $HCoRuOs_2(CO)_{13}$, and $HOs_3(CO)_{13}$. Mass spectral data for these three clusters, Table C, strongly support the formulations given. The spectrum of each cluster exhibits the parent ion followed by ions corresponding to successive loss of carbonyls and the hydrogen ligand, and a fragment consisting of only the tetrametallic framework is prominent in each spectrum. The isotopic distributions of the parent ions of $HCoRu_3(CO)_{13}$, $HCoRu_2Os(CO)_{13}$, and $HCoRuOs_2(CO)_{13}$ agree well with those calculated from isotopic abundances, but the parent ion of $HCoOs_3(CO)_{13}$ was not resolved well enough to allow comparison. The similarity of the infrared and electronic absorption spectra of these clusters, Table V, suggests similar structures for the four derivatives. The spectral blue shift in their electronic absorption spectra as the Os content increases is similar to that observed in the $H_2FeRu_3(CO)_{13}$, $H_2Fe-Ru_2Os(CO)_{13}$, and $H_2FeRuOs_2(CO)_{13}$ series,[1] consistent with the notion that the electronic transitions are between orbitals involved in the metal–metal bonding and that the strength of the overall M–M bonding increases with increasing Os content.

The $H_2FeRu_2Os(CO)_{13}$ and $H_2FeRuOs_2(CO)_{13}$ clusters previously studied were shown to exist as a mixture of two isomeric forms which readily interconvert.[1,24] In the static ^1H NMR spectra of each of the Fe–Ru–Os clusters, separate resonances due to each isomer were clearly apparent.[24] Likewise, the bridging CO region of the IR spectrum of each cluster showed a total of four bands, with two arising from each of the two isomers. In contrast, $HCoRu_2Os(CO)_{13}$ and $HCoRuOs_2(CO)_{13}$ show no evidence for isomers in their IR spectra, and each displays only a temperature-invariant (–80 ← 30 °C) singlet in the metal hydride region of their ^1H NMR spectra, Table VI.

On the basis of the insight gained from the crystal structure of $[PPN][CoRu_3(CO)_{13}]$, we suggest that the new clusters $HCoRu_3(CO)_{13}$, $HCoRu_2Os(CO)_{13}$, $HCoRuOs_2(CO)_{13}$, and $HCoOs_3(CO)_{13}$ have the basic structure shown in **5**, with three
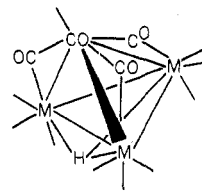
5

bridging CO's and with the hydride ligand triply-bridging the triangular face opposite the Co atom. No isomers, of course, can be drawn for such structures for $HCoRu_2Os(CO)_{13}$ and $HCoRuOs_2(CO)_{13}$, in full accord with their infrared and ^1H NMR spectra. Further evidence that the hydride ligands are associated with the Ru_xOs_{3-x} triangles comes from comparison of the ^1H NMR chemical shifts within the series $HCoRu_3(CO)_{13}$, $HCoRu_2Os(CO)_{13}$, and $HCoRuOs_2(CO)_{13}$. As the Os content of the cluster increases, the hydride resonances show an upfield shift of exactly the same magnitude, Table VI, as seen for the $H_2FeRu_3(CO)_{13}$, $H_2FeRu_2Os(CO)_{13}$, and $H_2FeRuOs_2(CO)_{13}$ series in which the hydride ligands are clearly bound to the Ru_xOs_{3-x} portion of the cluster. The lack of significant broadening of the hydride resonances also supports our contention that the hydride ligand is not associated with Co ($I = \,^7/_2$) but rather with the Ru_xOs_{3-x} triangle. Solution instability of these neutral clusters has prevented isolation of crystals suitable for crystallographic study, but the basic structure **5** is fully consistent with the available spectroscopic data.

---

(23) Geoffroy, G. L.; Gladfelter, W. L.; Bruck, M.; Bau, R., to be submitted for publication.
(24) Geoffroy, G. L.; Gladfelter, W. L. *J. Am. Chem. Soc.* **1977**, *99*, 6775.
(25) Gladfelter, W. L.; Geoffroy, G. L., submitted for publication.